

# Copper(II) Ion-Catalyzed and Molecular Packing-Dependent Dimerization of Pyridoxal 5-Phosphate–Pyridoxamine 5-Phosphate Schiff Base as a Structural Model for in Vitro Transformation of Amino Acid by Pyridoxal 5-Phosphate: X-Ray Crystal Structural Investigation

Toshimasa Ishida,\* Reijirou Manabe, Yasuko In, Hajime Takashima,<sup>†</sup> Kunihiro Kitamura,<sup>†</sup> and Akio Wakahara<sup>††</sup>

Osaka University of Pharmaceutical Sciences, 4-20-1 Nasahara, Takatsuki, Osaka 569-1094

<sup>†</sup>Research Center, Taisho Pharmaceutical Co., Ltd., 1-404 Yoshino-cho, Ohmiya 330-8530

<sup>††</sup>Fujisawa Pharmaceutical Co., Ltd., 2-1-6 Kashima, Yodogawa-ku, Osaka 532-8514

(Received November 18, 1998)

X-Ray crystal structures of the end products, obtained by in vitro Cu(II)-mediated transamination reaction of L-alanine by the vitamin B6 coenzyme, show that the Cu(II) complex of pyridoxal 5-phosphate–pyridoxamine 5-phosphate (PLP–PMP) Schiff base ( $\text{Cu}\cdot\text{C}_{16}\text{H}_{18}\text{N}_3\text{O}_{10}\text{P}_2$ , **1**) is spontaneously covalent-bonded between the azomethine carbons of two neighboring Schiff bases with the (*R,R*)- or (*S,S*)-configuration, and is led to a dimer structure of the *trans* (**2a**) or *cis* (**2b**) conformational isomer around the covalent bond, depending on the molecular packing in the crystal. Since crystals of **1** have been obtained, the C–C covalent bond could be formed at the crystalline state. Molecular orbital calculations suggest that the electronic structure of the Schiff base is significantly delocalized by the coordination of the copper(II) ion; also the vertical stacking of **1** aromatic rings, which is suitable for the dimer formation, is promoted by electrostatic interactions between the  $\text{P}_z$  orbitals of the azomethine nitrogen and carbon atoms. Based on the transformation of **1** to **2a/2b**, we propose a transition pathway via the aldimine or ketimine dimer form concerning the metal- and PLP-catalyzed biomimetic transformation of amino acid.

In addition to the coenzyme of a number of enzymes which catalyze different types of reactions in amino acid metabolism, it is well known that pyridoxal 5-phosphate (PLP) catalyzes the nonenzymatic transformation of amino acids to various products in vitro; the reaction mechanism has been analyzed in order to understand the enzymatic metabolism of amino acids.<sup>1–4</sup> For example, the PLP-catalyzed transamination of amino acids leads to the production of  $\alpha$ -keto acids and pyridoxamine 5-phosphate (PMP), where a divalent metal ion, such as Cu(II), accelerates the reaction. Since it has been proposed that selection of the transformation pathway of amino acid, such as decarboxylation, transamination or racemization, is highly related to the stereochemical aspect of PLP–amino acid Schiff base and its metabolite,<sup>5</sup> the conformational features have been studied for various types of Schiff bases.<sup>6,7</sup> As a series of our investigations on molecular conformations of various vitamin B6–amino acid Schiff bases,<sup>8–11</sup> **2a** was obtained as an end product in the Cu(II)- and PLP-mediated transamination experiment of L-alanine. This paper deals with its structural and conformational features, studied by an X-ray crystal analysis and a molecular orbital calculation. Previously, we reported on the X-ray crystal structure of **2b**,<sup>11</sup> which was

obtained from a similar, but not same, reaction condition, and had the same chemical formula as that of **2a**. X-ray crystal analyses showed that, although both compounds consisted of covalent-bonded dimers of the Cu(II): PLP–PMP Schiff base complex (**1**), they were conformational isomers about the covalent bond. Since the mechanism on the nonenzymatic vitamin B6-catalyzed transformation of amino acid is still within the imagination, the molecular and structural features of **2a** and **2b** could provide a structural basis for such a reaction scheme in vitro.<sup>1,4</sup> The chemical structures of **1** and **2**, together with the atomic numbering used in this work, are given in Fig. 1.

## Results and Discussion

**Molecular Structure.** The molecular conformation of **2a** is shown in Fig. 2; some selected bond lengths, angles, and torsion angles are given in Table 1.

**2a** consisted of the Cu(II) complex of the PLP–PMP Schiff base. The most striking structural feature of **2a** is unique dimer formation via covalent-bond formation between the azomethine carbons of two vertically stacked **1s**, in which the intramolecular conformation around the C(4')A–C(4')B bond is of the *trans*-type, the configuration at the (C(4')A,

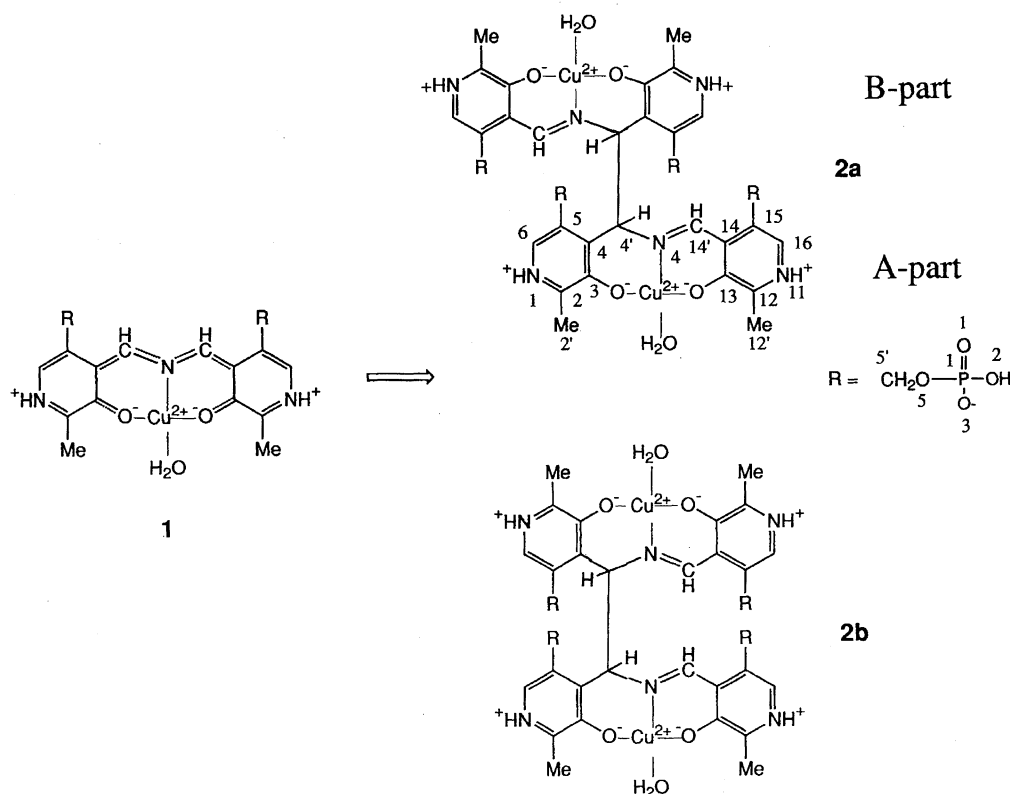


Fig. 1. Chemical structures of **1**, **2a**, and **2b**, together with the atomic numbering for **2a** A-part moiety used in this work. Two different crystals (**2a** and **2b**) have been obtained so far. Although both crystals have the same configurations at C(4')A, C(4')B, i.e., (*R,R*) or (*S,S*)-configuration, they are conformational isomers around the C(4')A–C(4')B bond, *trans* for **2a** and *cis* for **2b**; because of the steric hindrance, the free rotation around this bond is not allowed. The atomic numbering for **2a** B-part is the same as that for A-part. The atomic numbering for the phosphate (= R) is shown only for the left side of A-part. The numberings for other phosphates were done with the same manner.

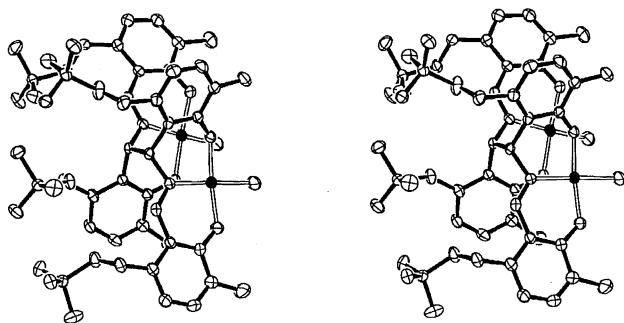


Fig. 2. A stereoscopic view of **2a** molecular conformation with the (*S,S*) configuration at the covalent-bonded C(4')-A and C(4')B atoms. Copper(II) ions are shown as filled ellipsoids, and open bond lines represent coordinations. H atoms are omitted for clarity. The bonding parameters of **2a** indicate that each phosphate oxygen is deprotonated, each pyridine nitrogen protonated and each pyridine phenolic oxygen deprotonated, and that the Schiff base is neutralized by two copper(II) ions coordinated with the square-planar pattern. Because of centrosymmetric space group of crystal **2a**, the dimers with the (*R,R*)-configuration are involved in pairs in the crystal.

C(4')B) position being either of (*R,R*)- or (*S,S*). Because **2a** has not been obtained in the absence of the copper(II) ion,

this result suggests that the metal ion catalyzes dimerization of **1s**, nonenzymatically, with the copper(II) ion acting as both the center for fixation of the Schiff base and an electronic activator of the azomethine carbon to facilitate spontaneous covalent-bond formation. Characteristically, the bond length of C(4')A–C(4')B [1.594(7) Å] is somewhat longer than the generally accepted value (1.542 Å)<sup>12)</sup> for the (C<sup>#</sup>)<sub>2</sub>–CH–CH–(C<sup>#</sup>)<sub>2</sub> bond sequence, where C<sup>#</sup> represents any Csp<sup>3</sup> atom, indicating the such a bonding state is energetically unstable due to a steric hindrance, together with the existence of a conformational isomer around this bond. Indeed, this bond is very susceptible to being broken, as evidenced by the lack of a mother ion peak and by the appearance of an intense peak corresponding to the monomer fragment in the mass spectrum of **2a**. Also, the *cis* isomer around the C(4')A–C(4')B bond has been observed for **2b**, respectively.

The Schiff base of **2a** is stabilized by the Cu(II) ion. The Cu(1)A ion is square-coordinated to the A-part Schiff base with four basal atoms being O(3)A [1.908(4) Å], N(4)A [1.960(4) Å], O(13)A [1.883(4) Å], and O(1W)A [2.000(4) Å]. The phenolic O(13)B of B-part Schiff base [2.528(4) Å] and O(6) of perchlorate ion [2.560(8) Å] interact with the copper ion from the apical direction by electrostatic interactions. Nearly the same coordination mode is also

Table 1. Selected Structural Parameters of **2a**<sup>a)</sup>

	A-part	B-part
Bond lengths		
C(3)–O(3)	1.326(6) Å	1.322(6) Å
C(13)–O(13)	1.289(7)	1.279(7)
C(4)–C(4')	1.511(7)	1.510(7)
C(14)–C(14')	1.464(7)	1.449(7)
C(4')–N(4)	1.486(6)	1.476(6)
N(4)–C(14')	1.486(6)	1.476(6)
C(4')A–C(4')B	1.594(7) Å	
Bond angles		
C(4)–C(4')–N(4)	112.6(3)°	111.4(3)°
C(4')B–C(4')A–C(4)A/C(4')A–C(4')B–C(4)B	111.1(3)	110.7(3)
C(4')B–C(4')A–N(4)A/C(4')A–C(4')B–N(4)B	113.1(3)	113.2(3)
C(4')–N(4)–C(14')	114.6(3)	116.4(3)
C(14)–C(14')–N(4)	124.9(3)	124.7(3)
Torsion angles		
C(4)–C(4')–N(4)–C(14')	141.0(5)°	124.8(5)°
C(4')–N(4)–C(14')–C(14)	175.3(6)	178.4(6)
C(4)A–C(4')A–C(4')B–C(4)B	153.3(4)°	
C(4)A–C(4')A–C(4')B–N(4)B	27.4(4)	
N(4)A–C(4')A–C(4')B–C(4)B	25.6(4)	
N(4)A–C(4')A–C(4')B–N(4)B	–100.2(4)	

a) The suffix letters A and B represent A and B parts of **2a**, respectively.

formed between the Cu(1)B atom and the B-part Schiff base: O(3)B [1.900(4) Å], N(4)B [1.956(4) Å], O(13)B [1.912(4) Å], O(1W)B [2.027(4) Å], O(3)A [2.335(4) Å], and O(11) [2.91(1) Å]. This kind of bipyramidal-like coordination has frequently been observed in the related Schiff bases.<sup>13)</sup>

#### Unique Packing of Phosphate Groups in the Crystal.

The packing mode of **2a** complexes is schematically shown in Fig. 3. Possible hydrogen bonds and electrostatic atomic pairs are summarized in Table 2.

In the crystal structure, the layers of **2as** parallel to (0 1 0) are stacked and stabilized by hydrogen bonds or electrostatic interactions with water molecules, copper(II) and perchlorate ions, which are located among the layers. As is obvious from Fig. 3, the interaction mode between the neighboring layers is different at the upper and lower sides of the central layer, due to piling up of **2as** along the *c*-direction with the same orientation; this is in contrast with the nearly same interaction mode at both sides of the stacking later of **2bs**, in which the alternative complexes were antiparallely piled up.<sup>11)</sup> Four phosphates in **2a**, eight water solvents [O(3)W–O(7)W, O(9)W–O(11)W] and one perchloride ion [Cl(1), O(1)–O(4)] are all in the upper space and arranged along to the *a*-direction, thus forming an anionic environment. Three copper(II) ions [Cu(3)–Cu(5)] are located in this space and stabilize the space by electronic neutralization and coordination to the polar atoms; Cu(3) and Cu(4) are located on the center of symmetry and participate in fixation of the phosphate groups through coordination: Cu(3)–O(12P)B = 1.914(4) Å, Cu(3)–O(3)W = 1.946(4) Å, Cu(4)–O(12P)A = 1.925(4) Å, Cu(4)–O(13P)B = 1.968(4) Å. On the other hand, the lower space is created by the

cluster of water molecules and stabilized by the intermolecular hydrogen bonds [O(1)WA, O(1)WB, O(8)W, O(12)W, O(13)W]. The perchloride ions [Cl(2), O(5)–O(8), Cl(3), O(9)–O(12), Cl(4), O(13)–O(16)] are also located in this space and stabilize the layers of **2as** piling up to the *c*-direction through the hydrogen bonds to the polar atoms of **2a** and water molecules.

Characteristically, all phosphate groups in **2a** exist in the space of the same side. The crystal packing shows a reason to force the phosphate groups to gather at the same side. The Cu(3)/Cu(4) ions, labeled in Fig. 3, play a role of linking the centrosymmetrically-translated phosphate groups of the A- and B-parts [P(11), O(11P)–O(13P)] through coordination bonds. The remaining phosphates [P(1), O(1P)–O(3P)] are forced to take the same orientation as the result of square-coordinations of Cu(1)A and Cu(1)B to the respective O(3) and O(13) atoms of **2a**; Cu(5) ions locate in the vicinity of these phosphates and neutralize their anionic charges.

#### Stereoselective Dimer Formation Catalyzed by Copper(II) Ion.

Previously, we reported on the crystal structure of **1**,<sup>10)</sup> the chemical structure of which closely resembles an intermediate state between the aldimine and ketimine forms of the Cu(II) complex of the PLP–PMP Schiff base (Fig. 4); also the short contacts of ca. 2.3 Å were observed between the azomethine carbons of the vertically and antiparallely stacked **1s**. When the crystal structure of **2b**, which consists of the *cis*-dimers with the (*R,R*)/(*S,S*)-configuration at [C(4')A, C(4')B], is compared with that of **1**, it is obvious that the covalent-bond formation takes place at the crystalline state. On the other hand, the present X-ray analysis indicates that **2a** corresponds to the *trans*-dimer

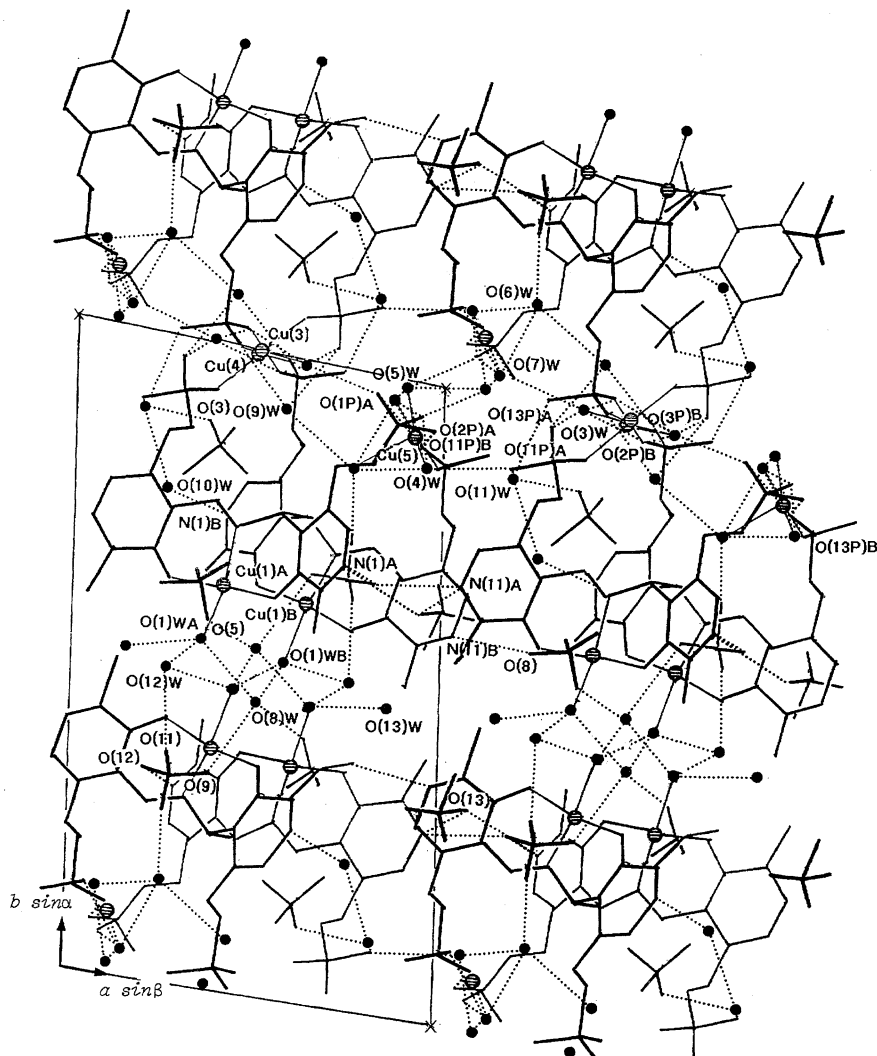


Fig. 3. Schematic crystal packing of **2a**s and their interactions with water molecules, copper(II) and perchlorate ions. Water molecules and copper(II) ions are represented with the filled and shaded circles, respectively. The O(1)—O(4), O(5)—O(8), O(9)—O(12), and O(13)—O(16) atoms of four perchlorate anions are bonded to Cl(1), Cl(2), Cl(3) and Cl(4), respectively. Possible hydrogen bonds and coordination bonds are shown with dotted and thin lines, respectively. A box enclosed with thin lines represent one unit cell, viewed from the *c*-axis.

structure of **1** with the (*R,R*)/(*S,S*)-configuration at [C(4')A, C(4')B]. We believe that the covalent-bond formation in **2a** also proceeds via a crystalline state in which **1**s are vertically and parallelly stacked, although such crystals have not yet been isolated.

Based on these X-ray results, a discussion about the transformation pathway from **1** to **2a** or **2b** is possible. Provided that the dimerization takes place between the azomethine carbons of the stacked **1**s, four different geometrical isomers and their enantiomers are possible for the dimerization of **1** (Fig. 5), depending upon the combination of the *cis/trans*-isomer around the C(4')A–C(4')B or C(14')A–C(14')B bond and the *R/S*-configuration at the covalent-bonded atoms, i.e., *trans*-(*RR*)(*SS*) (**2a**), *trans*-(*RS*)(*SR*), *cis*-(*RR*)(*SS*) (**2b**), and *cis*-(*RS*)(*SR*). As depicted in Fig. 5(a), for example, the (*cis*, *R,S*) isomer could be produced when a covalent bond is formed between the same C(4') atoms of the parallelly overlapped **1**s. On the other hand, covalent-bond formation be-

tween the same C(4') atoms of antiparallely overlapped **1**s could lead to the formation of the (*cis*, *R,R*) isomer. Simultaneous covalent bond formations at C(4')A–C(4')B and C(14')A–C(14')B atomic pairs would be impossible because of the energetically unfavorable [3+3] cycloaddition. Based on these considerations, it is reasonable to propose that crystals **2a** and **2b** are produced by the transformation pathways of Figs. 5(c) and (d) and Figs. 5(e) and (f), respectively. Furthermore, it may be said that dimerization from **1** to **2a** or **2b** occurs efficiently via the solid state and that the stereospecificity is dependent upon the packing mode between the monomers, which is dominated by interactions with the surrounding metal ions, counter ions, and solvent molecules.

#### Effect of Copper(II) Ion on the C(4')/C(14') Atomic Charge.

The crystal structures of **2a** and **2b** indicate that the copper(II) ion induces spontaneous dimerization of the PLP–PMP Schiff base. This would imply that the C(4') and C(14') electrons of the Schiff base, which participate in

Table 2. Possible Hydrogen Bonds<sup>a)</sup> and Short Contact Atomic Pairs (< 3.0 Å)

Donor	Acceptor	Distance (Å)	Symmetry operation of Acceptor
Hydrogen bond			
N(1)A	O(12)	2.95(2)	$1-x, -y, 2-z$
N(1)A	O(13)	2.98(2)	$2-x, -y, 1-z$
O(2P)A	O(11P)B	2.502(7)	$x, y, z$
N(11)A	O(12)	2.95(2)	$-x, -y, 1-z$
N(11)A	O(13)	3.02(2)	$1-x, -y, 1-z$
O(11P)A	O(4W)	2.726(7)	$x-1, y, z$
O(11P)A	O(11W)	2.541(9)	$1-x, -y, 1-z$
O(1W)A	O(8W)	2.809(7)	$x, y-1, z$
O(1W)A	O(12W)	2.857(9)	$x, y-1, z$
O(1W)A	O(13W)	2.96(1)	$1-x, -y, 1-z$
N(1)B	O(10W)	2.774(9)	$1-x, -y, 1-z$
N(11)B	O(8)	2.92(2)	$x+1, y, z$
O(1P)B	O(11W)	3.020(9)	$x, y, z$
O(11P)B	O(1P)A	2.636(6)	$x, y, z$
O(1W)B	O(1W)B	2.755(7)	$1-x, -1-y, 1-z$
O(1W)B	O(8W)	2.716(7)	$x, y-1, z$
O(1W)B	O(12W)	2.904(9)	$1-x, -y, 1-z$
O(3W)	O(1P)A	2.794(6)	$1-x, -y, 2-z$
O(3W)	O(13P)A	2.822(7)	$x, y, z$
O(3W)	O(2P)B	2.707(7)	$x, y, z$
O(3W)	O(2P)B	2.762(7)	$1-x, -y, 2-z$
O(4W)	O(3P)A	2.617(6)	$x, y, z-1$
O(4W)	O(13P)B	2.678(6)	$x, y, z$
O(4W)	O(5W)	2.814(6)	$x, y, z$
O(4W)	O(6W)	2.972(7)	$x, y, z$
O(5W)	O(3P)A	2.619(6)	$x, y, z-1$
O(5W)	O(13P)A	2.616(6)	$1-x, -y, 1-z$
O(5W)	O(5W)	3.044(6)	$2-x, -y, 1-z$
O(5W)	O(7W)	2.741(7)	$x, y, z$
O(6W)	O(10)	2.98(1)	$1-x, -y, 1-z$
O(6W)	O(7W)	3.096(8)	$x, y, z$
O(6W)	O(9W)	2.771(8)	$x, y, z$
O(7W)	O(3P)A	2.895(7)	$2-x, -y, 1-z$
O(7W)	O(11P)B	2.721(7)	$x, y, z$
O(7W)	O(13P)B	2.861(7)	$x, y, z$
O(8W)	O(5)	2.80(1)	$1-x, -y, 2-z$
O(8W)	O(9)	2.89(1)	$x, y, z$
O(9W)	O(13P)A	2.723(7)	$1-x, -y, 1-z$
O(9W)	O(3P)B	3.039(7)	$1-x, -y, 1-z$
O(9W)	O(3)	3.01(1)	$1-x, -y, 1-z$
O(10W)	O(11W)	3.02(1)	$x, y, z$
O(11W)	O(3)	3.04(1)	$x, y, z$
O(12W)	O(11)	2.86(2)	$x, y, z$
Short contact atomic pair			
O(3)A	O(3)B	2.919(6)	$x, y, z$
N(4)A	O(3)B	2.967(6)	$x, y, z$
O(12P)A	O(3P)B	2.732(5)	$x, y, z$
O(12P)A	O(3P)B	2.780(6)	$1-x, -y, 1-z$
O(12)	O(13)	2.57(2)	$x-1, y, z$

a) The identification of donor and acceptor atoms between water molecules is tentative.

covalent-bond formation, are significantly activated by coordination of the copper(II) ion for the transformation of **1** to **2a** or **2b**. To estimate which kind of electron is most affected, molecular orbital calculations<sup>14)</sup> were performed for

the PLP–PMP Schiff base and its Cu(II) complex. Some selected results are given in Table 3. A bond order analysis<sup>15)</sup> indicated that the  $\pi$ -electrons on the PLP–PMP Schiff base are significantly delocalized by coordination of the Cu(II) ion,

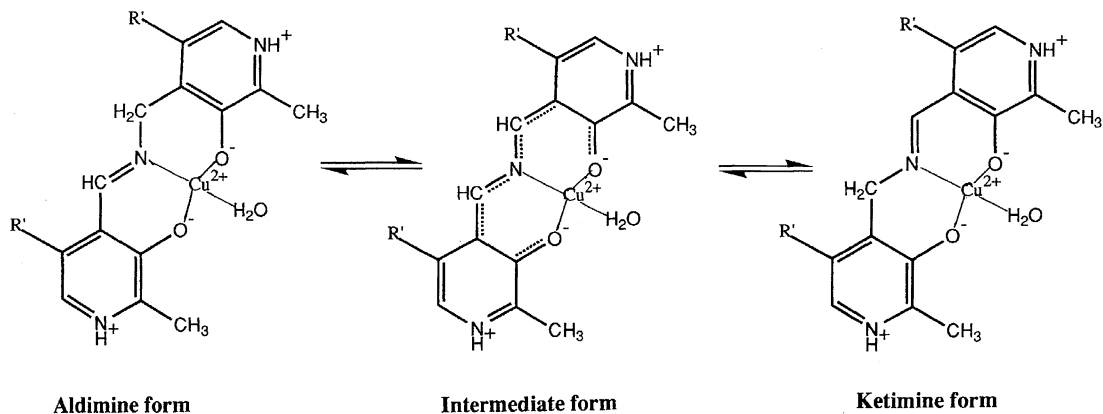


Fig. 4. Aldimine, ketimine and their intermediate structures of Cu(II) complex of PLP-PMP Schiff base.

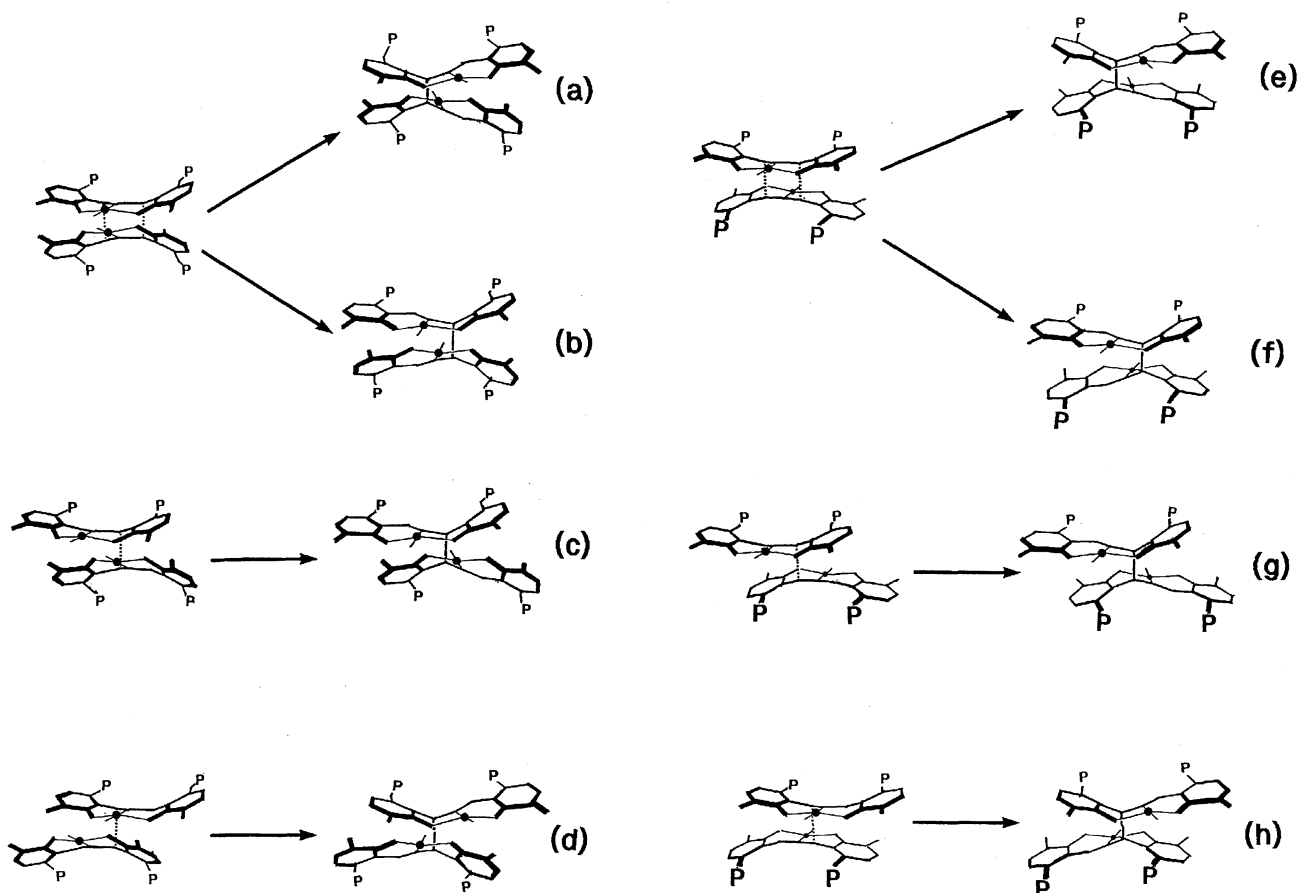


Fig. 5. Four possible geometrical isomers and their respective enantiomers by the dimerization of **1** with *cis*-(*R,S*) (a), *cis*-(*S,R*) (b), *trans*-(*S,S*) (c), *trans*-(*R,R*) (d), *cis*-(*R,R*) (e), *cis*-(*S,S*) (f), *trans*-(*S,R*) (g), or *trans*-(*R,S*) (h) configuration. These isomers are formed by a covalent-bond formation between the two parallelly [for (a)–(d)] or antiparallelly [for (e)–(h)] stacked **1** monomers at the intermolecular C(4')A–C(4')B [(a) and (e)], C(14')A–C(14')B [(b) and (f)], C(4')A–C(14')B [(c) and (g)], or C(14')A–C(4')B [(d) and (h)] atomic pair. The crystals of **2a** and **2b** consist of isomers of (c)/(d) and (e)/(f), respectively. The thick and thin lines express the front and back sides of the structures, respectively. The letter P represents phosphate group.

leading to stabilization of the planar structure of the Schiff base. On the other hand, the atomic charges of C(4'), N(4), and C(14') on their  $\phi_{2p_z}$  orbitals, which would correspond to  $\pi$ -electrons that participate directly in the  $\sigma$ -covalent-bond formation, are reversely localized by the copper coordination. This result may explain why **1s** prefer to stack themselves perpendicular to the aromatic plane: the electrostatic

interactions between the neighboring N(4) and C(4')/C(14') atoms are increased by coordination of the copper(II) ion. These data, though not definitive, support the positive contribution of the Cu(II) ion for dimerization of the PLP-PMP Schiff base.

**PLP- and Cu(II)-Catalyzed Transformation of Amino Acid.** As stated above, the chemical/electronic

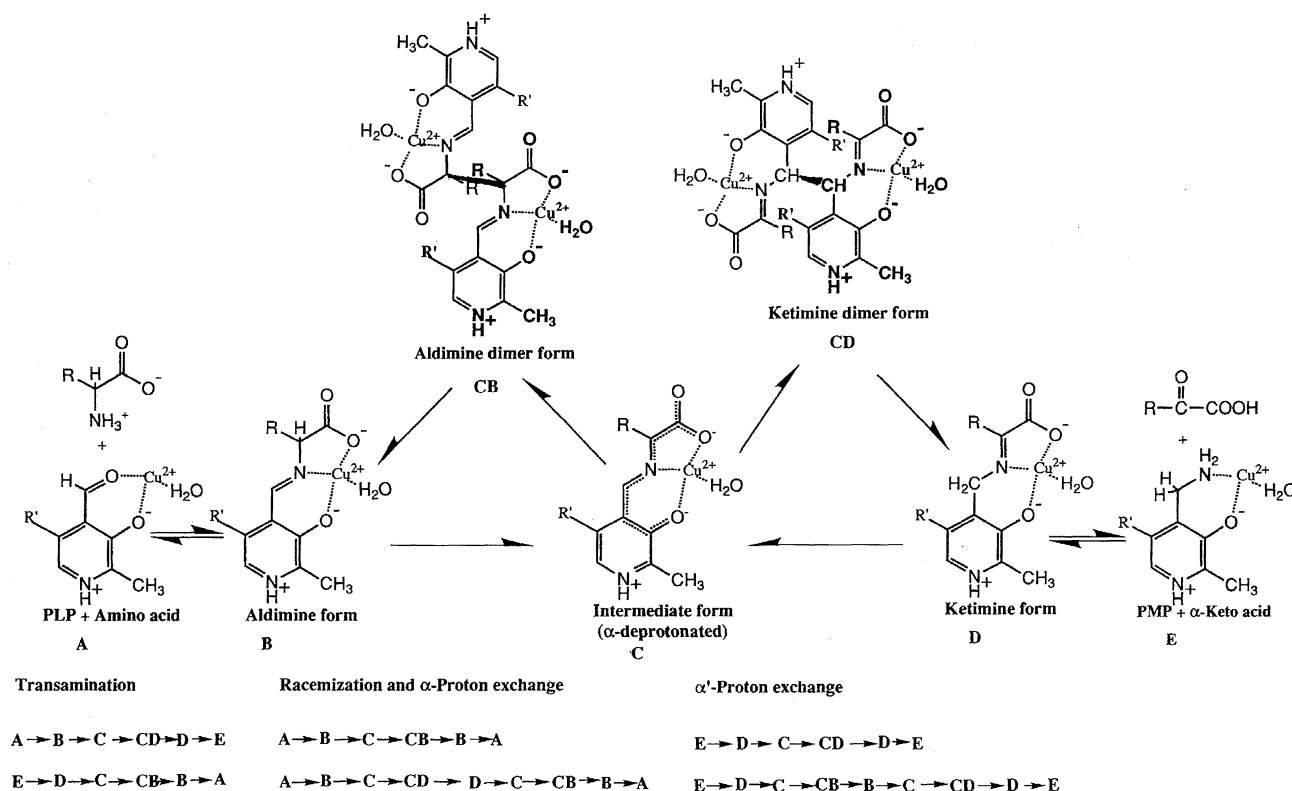


Fig. 6. PLP- and Cu(II)-catalyzed transformation of amino acid. The respective reaction pathways for transamination, racemization, and α-proton exchange and α'-proton exchange are shown by A—E. The letters R and R' represent the amino acid side chain and the phosphate group, respectively.

Table 3. π-Bond Orders and Pz Orbital Atomic Electrons of PLP-PMP and PLP-PMP·Cu(II)

π-Bond order	PLP-PMP·Cu	PLP-PMP
C(4)–C(4')	1.246	1.212
C(4')–N(4)	1.400	1.367
N(4)–C(14')	1.487	1.494
C(14')–C(14)	1.195	1.175
C(3)–O(3)	1.459	1.681
C(3)–C(4)	1.215	1.058
C(13)–O(13)	1.425	1.723
C(13)–C(14)	1.237	1.064
Atomic electrons of Pz orbitals		
	PLP-PMP·Cu	PLP-PMP
C(4)	1.081	1.067
C(4')	0.916	1.005
N(4)	1.245	1.161
C(14')	0.933	1.016
C(14)	1.068	1.054

structure<sup>10</sup> (Fig. 1) of **1** closely resembles the intermediate state (Fig. 4) between the aldimine and ketimine structures of the PLP-amino acid Schiff base<sup>1–4</sup> [an important intermediate structure in various transformation, such as transamination, racemization, and α- or α'-proton exchange, of amino acid catalyzed by PLP (Fig. 6)]. On the other hand, the structure of **2a/2b** simulates the aldimine/ketimine form of the PLP-amino acid Schiff base and suggests the Cu(II)-

mediated transformation of **1** → **2a/2b**. Therefore, the conformational and stereochemical features of **1**, **2a**, and **2b** would provide a possible structural basis for a nonenzymatic transformation mechanism of amino acid by PLP.

As for the question of how the transition from **C** to **B** and **D** in Fig. 6 is structurally accomplished, the crystal structures of **2b** and **2a** propose a transition pathway via the aldimine (**CB**) and ketimine (**CD**) dimer forms, respectively. It is widely accepted that the intermediate **C** is directly transformed from **B**, as a result of the abscission of C<sub>α</sub>–H, caused by a strong electron-withdrawal effect of the metal and pyridine NH cations. As judged from the X-ray crystal structures, the molecular orbital calculations, and the possible formation pathways (Fig. 5) of **2a** and **2b**, it is possible that (i) two **C** molecules stack themselves perpendicular to the plane, (ii) the ability of the azomethine carbon of **C** to form a covalent bond with that of the partner is elevated by the copper(II) ion, and then (iii) the dimerization between the neighboring C<sub>α</sub> atoms (**CB**) or C<sub>α'</sub> atoms (**CD**) is spontaneously formed. As indicated in the crystal structure of **2a/2b**, the C<sub>α</sub>–C<sub>α'</sub>/C<sub>α'</sub>–C<sub>α'</sub> bond of **CB/CD** would be very unstable, because R (side chain of amino acid) is much more bulky than the H atom of **2**, thus leading to bond disruption and regeneration with the H<sup>+</sup> ion.

## Experimental

**Preparation.** The PLP-PMP Schiff base was synthesized according to a previously described method.<sup>16,17</sup> To an aqueous solution of the Schiff base (10 mM, 1 M = 1 mol dm<sup>–3</sup>), equimolar

Cu(ClO<sub>4</sub>)<sub>2</sub> was added. The solution was stirred at room temperature (ca. 20 °C) for a period of a few weeks, during which time the cover of the container was left slightly open to allow slow evaporation of the solvent. Greenish plate crystals of **2a** precipitated from the reaction solution within 1–2 weeks. Since the same solution, except without Cu(ClO<sub>4</sub>)<sub>2</sub>, showed no UV spectral change, the production of **2a** is clearly copper-dependent.

**X-Ray Crystal Analysis.** A single crystal with dimensions 0.4×0.2×0.05 mm was used for X-ray diffraction data collection on a Rigaku AFC-5 diffractometer employing graphite-monochromated Cu K $\alpha$  radiation. The crystal data are as follows: (Cu·C<sub>16</sub>H<sub>18</sub>N<sub>3</sub>O<sub>10</sub>P<sub>2</sub>)<sub>2</sub>·2Cu(ClO<sub>4</sub>)<sub>2</sub>·13H<sub>2</sub>O, *M*<sub>r</sub> = 1834.76, triclinic, *P* $\bar{1}$ , *a* = 13.2550(9), *b* = 22.190(2), *c* = 11.848(1) Å,  $\alpha$  = 98.902(7)°,  $\beta$  = 107.522(6)°,  $\gamma$  = 100.322(4)°, *V* = 3187.5(4) Å<sup>3</sup>, *Z* = 2, *D*<sub>calcd</sub> = 1.912 g cm<sup>−3</sup>,  $\lambda$  (Cu K $\alpha$ ) = 1.5418 Å,  $\mu$ (Cu K $\alpha$ ) = 5.10 cm<sup>−1</sup>, *F*(000) = 1864. A total of 10679 independent reflections within 2 $\theta$  = 130° were collected in an  $\omega$ –2 $\theta$  scan mode and corrected for the Lorentz and polarization factors, and for the absorption effect. Of these, 8329 reflections with *I* > 2 $\sigma$ (*I*) were used for the structure refinement. The structure was solved by the heavy atom method and refined by the full-matrix least-squares method (SHELXL-93 program<sup>18)</sup>) with the use of anisotropic temperature factors. The positions of H atoms were obtained from a difference Fourier map and included in the calculation of the structure factors. The function  $\sum w(F_o^2 - F_c^2)^2$  was minimized, where  $w = [\sigma(F_o^2)^2 + (0.0955p)^2 + 16.8510p]^{-1}$  and  $p = (F_o^2 + 2F_c^2)/3$ . The discrepancy indexes, *R* and *R*<sub>w</sub>, are 0.0529 and 0.1446 (0.0689 and 0.1597 for all reflections), respectively;<sup>19)</sup> no. of variables = 896, *S* = 0.927,  $\Delta/\text{esd}_{\text{max}} = 0.327$ ,  $\Delta/\text{esd}_{\text{mean}} = 0.021$ ,  $\Delta\rho_{\text{max}} = 1.357$  e Å<sup>−3</sup> and  $\Delta\rho_{\text{min}} = -1.013$  e Å<sup>−3</sup>.

**Molecular Orbital Calculation.** The atomic coordinates for PLP–PMP and PLP–PMP·Cu were prepared from the crystal structure of **1**.<sup>10)</sup> Molecular orbital calculations at the Hartree–Fock level were performed using the Gaussian94 program,<sup>14)</sup> where the 3-21 G basis set was used. An analysis of each bond order was performed by the Lowdin method.<sup>15)</sup>

## References

- 1) A. E. Martell, in "Advances in Enzymology," ed by A. Meister, John Wiley & Sons, New York (1982), Vol. 53, pp. 163–199.
- 2) "Transaminases," ed by P. Christen and D. E. Metzler, John Wiley & Sons, New York (1984).
- 3) D. L. Leussing, in "Vitamin B<sub>6</sub>, Pyridoxal Phosphate, Chemical, Biochemical and Medical Aspects, Part A," ed by D. Dolphin, R. Poulson, and O. Avramovic, John Wiley & Sons, New York (1986), pp. 69–115.
- 4) A. E. Martell, *Acc. Chem. Res.*, **22**, 115 (1989).
- 5) H. C. Dunathan, *Adv. Enzymol. Relat. Area Mol. Biol.*, **35**, 79 (1971).
- 6) M. M. Palcic and H. G. Floss, in "Vitamin B<sub>6</sub>, Pyridoxal Phosphate, Chemical, Biochemical and Medical Aspects, Part A," ed by D. Dolphin, R. Poulson, and O. Avramovic, John Wiley & Sons, New York (1986), pp. 25–68.
- 7) M. Darriet, M. J. Basurko, A. Cassaigne, and J. Darriet, in "Vitamin B<sub>6</sub>, Pyridoxal Phosphate, Chemical, Biochemical and Medical Aspects, Part A," ed by D. Dolphin, R. Poulson, and O. Avramovic, John Wiley & Sons, New York (1986), pp. 265–307.
- 8) T. Ishida, K. Hatta, S. Yamashita, M. Doi, and M. Inoue, *Chem. Pharm. Bull.*, **34**, 3553 (1986).
- 9) H. Nagata, M. Doi, M. Inoue, T. Ishida, M. Kamigauchi, M. Sugiura, and A. Wakahara, *J. Chem. Soc., Perkin Trans. 2*, **1994**, 983.
- 10) T. Ishida, Y. In, H. Nagata, M. Doi, and A. Wakahara, *Chem. Lett.*, **1995**, 1137.
- 11) T. Ishida, Y. In, C. Hayashi, R. Manabe, and A. Wakahara, *Bull. Chem. Soc. Jpn.*, **70**, 2375 (1997).
- 12) F. H. Allen, O. Kennard, D. G. Watson, L. Brammer, A. G. Orpen, and R. Taylor, *J. Chem. Soc., Perkin Trans. 2*, **1987**, S1.
- 13) M. Darriet, M. J. Basurko, A. Cassaigne, and J. Darriet, in "Vitamin B<sub>6</sub>, Pyridoxal Phosphate, Chemical, Biochemical and Medical Aspects, Part A," ed by D. Dolphin, R. Poulson, and O. Avramovic, John Wiley & Sons, New York (1986), pp. 265–307.
- 14) M. J. Frisch, G. W. Trucks, H. B. Schlegel, P. M. W. Gill, B. G. Johnson, M. A. Robb, J. R. Cheeseman, T. Keith, G. A. Petersson, J. A. Montgomery, K. Raghavachari, M. A. Al-Laham, V. G. Zakrzewski, J. V. Ortiz, J. B. Foresman, J. Cioslowski, B. B. Stefanov, A. Nanayakkara, M. Challacombe, C. Y. Peng, P. Y. Ayala, W. Chen, M. W. Wong, J. L. Andres, E. S. Replogle, R. Gomperts, R. L. Martin, D. J. Fox, J. S. Binkley, D. J. Defrees, J. Baker, J. P. Stewart, M. Head-Gordon, C. Gonzalez, and J. A. Pople, "Gaussian 94, Revision D.4," Gaussian, Inc., Pittsburgh, PA (1995).
- 15) A. B. Sannigrahi and T. Kar, *J. Chem. Educ.*, **65**, 674 (1988).
- 16) M. Ikawa, *Arch. Biochem. Biophys.*, **118**, 497 (1967).
- 17) F. Nepveu, J.-J. Bonnet, and J.-P. Laurent, *J. Coord. Chem.*, **11**, 185 (1981).
- 18) G. M. Sheldrick, "SHELXL-93: A Program for the Refinement of Crystal Structures from Diffraction Data," University of Göttingen (1993).
- 19) Lists of atomic coordinates, anisotropic thermal parameters, bond lengths, bond angles, torsion angles, the coordination parameters around the copper ion, and observed and calculated structure factors are deposited as Document No. 72016 at the Office of the Editor of Bull. Chem. Soc. Jpn.